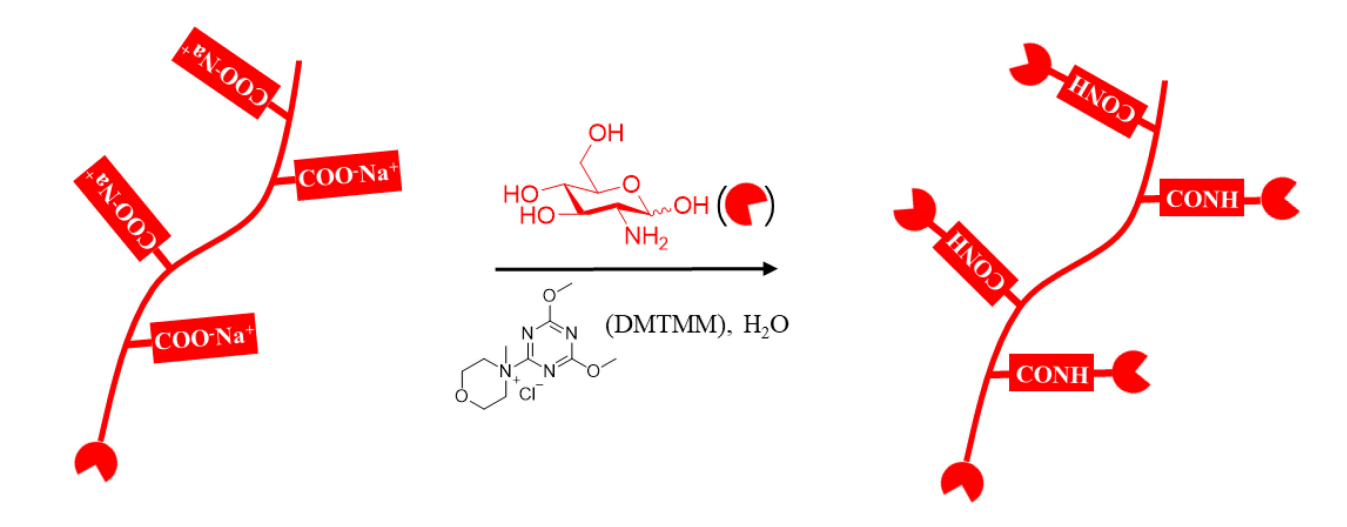
Synthesis and characterization of multi-reducing end

2 polysaccharides

- 3 Zhenghao Zhai‡, Yang Zhou‡, Andrew G. Korovich, Brady A. Hall, Hu Young Yoon, Yimin
- 4 Yao, Junchen Zhang, Michael J. Bortner, Maren Roman, Louis A. Madsen, and Kevin J. Edgar*
- 5 KEYWORDS: Reducing ends, multi-reducing end polysaccharides, cellulose, dextran, alginate,
- 6 hydrogel

7



Natural polysaccharides (only one reducing end per chain)

Multi-reducing end polysaccharides

9

8

10

13

14

15

16

17

18

19

20

21

22

23

24

25

26

27

28

29

30

31

32

33

ABSTRACT

Site-specific modification is a great challenge for polysaccharide scientists. Chemo- and regioselective modification of polysaccharide chains can provide many useful natural-based materials and help us illuminate fundamental structure-property relationships of polysaccharide derivatives. The hemiacetal reducing end of a polysaccharide is in equilibrium with its ring-opened aldehyde form, making it the most uniquely reactive site on the polysaccharide molecule, ideal for regioselective decoration such as imine formation. However, all natural polysaccharides, whether they are branched or not, have only one reducing end per chain, which means that only one aldehyde-reactive substituent can be added. We introduce a new approach to selective functionalization of polysaccharides as an entrée to useful materials, appending multiple reducing ends to each polysaccharide molecule. Herein we reduce the approach to practice using amide formation. Amine groups on monosaccharides such as glucosamine or galactosamine can react with carboxyl groups of polysaccharides, whether natural uronic acids like alginates, or derivatives with carboxyl-containing substituents such as carboxymethyl cellulose (CMC) or carboxymethyl dextran (CMD). Amide formation is assisted using the coupling agent 4-(4,6-dimethoxy-1,3,5triazin-2-yl)-4-methylmorpholinium chloride (DMTMM). By linking the C2 amines of monosaccharides to polysaccharides in this way, a new class of polysaccharide derivatives possessing many reducing ends can be obtained. We refer to this class of derivatives as multireducing end polysaccharides (MREPs). This new family of derivatives creates the potential for designing polysaccharide-based materials with many potential applications, including in hydrogels, block copolymers, pro-drugs, and as reactive intermediates for other derivatives.

37

38

39

40

41

42

43

44

45

46

47

48

49

50

51

52

53

54

55

56

57

INTRODUCTION

Nature freely provides us with polysaccharides in great abundance and variety from natural building blocks like CO₂ and water, in the presence of sunlight and oxygen. Polysaccharides are also attractive since they tend to be benign and are always biodegradable materials. Polysaccharides and their derivatives support an enormous variety of applications, including in biomedicine as components of vaccines, 1,2 as functional drug delivery excipients, 3-5 and as tissue engineering scaffolds.^{6,7} Polysaccharides can contribute useful properties by reacting with other biomacromolecules. For example, solubility, stability, and elimination half-life of protein drugs can be improved by conjugation with polysaccharides. However, the lack of regioselectivity of current methods can lead to non-uniform structures and poor reproducibility, which impede structure-property understanding, and are adverse for future commercialization. Therefore, regioand chemoselective chemical modification of polysaccharides is an important but challenging task. All polysaccharides possess multiple chemically nonequivalent but similar alcohols, and sometimes other reactive groups (e.g., carboxyls, amines, amides). These characteristics complicate the task of targeting specific hydroxyls or types of hydroxyls for chemical modification. 10,11 Aldehydes, like that of the anomeric carbon at the reducing end of polysaccharides, are particularly useful since their reactivity differs from that of all other polysaccharide carbons. For example, aldehydes can condense with amines to form imines, or can be reductively aminated to form amines.¹² Periodate oxidation is commonly used to create additional reactive sites on the polysaccharide for reaction, e.g., with amines, by which polysaccharide vicinal diols are cleaved to dialdehydes, thereby opening monosaccharide rings. This method is efficient and has been applied to many polysaccharides including cellulose, ^{13–15}

dextran, 16 amylose, 17,18 xanthan, 19 glycosaminoglycans, 20,21 and alginate. 22,23 These oxidized polysaccharides can be further reacted with amines to form imines. This is a convenient method for conjugating some small functional molecules, such as amino acids or proteins,²⁴ or forming hydrogels with amine-containing polymers.²⁵ However, periodate oxidation impacts higher order polysaccharide structure, decreases degree of polymerization (DP), and increases polysaccharide instability, leading to degraded mechanical properties.²⁶ Each natural polysaccharide, whether linear or branched, has one and only one reducing end, with its anomeric carbon that (for aldose-based polysaccharides) is in equilibrium between a ringclosed hemiacetal and an open-chain aldehyde form. Reducing end modification has been used to cellulose nanocrystals, 27,28 modify polysaccharides selectively, such manv as glycosaminoglycans, ^{29,30} dextran, ^{31,32} alginate, ³³ and chitosan. ^{34,35} However, since there is only one reducing end per polysaccharide chain, only one substituent per molecule can be attached in this way. Therefore, to obtain higher degree of substitution (DS) derivatives by regioselective aldehyde reactions, we considered whether it was possible and practical to introduce additional reducing ends to the polysaccharide chain, ideally while preserving DP, stability, and desirable physical properties. Herein we propose a new method to introduce multiple reducing ends to each polysaccharide molecule through coupling between carboxylic acids and amines. Carboxylic acid groups are common features of many natural polysaccharides, particularly those containing uronic acid monosaccharides, such as alginate, hyaluronic acid, and pectin. Polysaccharide derivatives bearing carboxylic acid substituents are also common, including carboxymethylated polysaccharides such as carboxymethyl cellulose (CMC) and carboxymethyl dextran (CMD). D-(+)-Glucosamine and D-(+)-galactosamine were chosen as models to demonstrate the introduction of reducing ends to

58

59

60

61

62

63

64

65

66

67

68

69

70

71

72

73

74

75

76

77

78

79

polysaccharides. We hypothesized that the carboxyl groups of polysaccharides (e.g., alginate, CMC, or CMD) could react with the 2-deoxy-2-amino groups of glucosamine or galactosamine assisted by a coupling agent such as 4-(4,6-dimethoxy-1,3,5-triazin-2-yl)-4-methylmorpholinium chloride (DMTMM), thereby attaching the monosaccharide bearing its added reducing end through an amide linkage. Because the newly formed amide linkage would be through C2 of the added monosaccharide, its reducing end (C1) would be introduced intact to the polysaccharide derivative. This approach would produce a new family of polysaccharide derivatives, which we propose to describe as multi-reducing end polysaccharides (abbreviated as MREPs). We describe herein our efforts to prove this hypothesis.

EXPERIMENTAL SECTION

Materials and Chemicals. Carboxymethyl cellulose sodium salt (CMCNa, degree of substitution of carboxymethyl group DS(CM) 0.84, calculated by ¹H NMR (Fig. S1); M_n = 1.14×10⁵ g/mol, determined by aqueous SEC), was from TCI. Carboxymethyl dextran sodium salt (CMDNa, DS(CM) 0.22, determined by ¹H NMR spectroscopy, Fig. S2; M_n = 1.27×10⁴ g/mol, determined by aqueous SEC), 4-(4,6-dimethoxy-1,3,5-triazin-2-yl)-4-methylmorpholinium chloride (DMTMM), and D-(+)-glucosamine hydrochloride (GlcN:HCl) were from Sigma-Aldrich. D-(+)-Galactosamine hydrochloride (GalN:HCl) was from Chem-Impex International. Alginic acid sodium salt (M/G ratio 1.9, determined by ¹H NMR spectroscopy, Fig. S3; M_n = 1.09×10⁵ g/mol, determined by aqueous SEC) and 1, 3, 4, 6-tetra-*O*-acetyl-D-glucosamine hydrochloride (acetyl-GlcN:HCl) were from Alfa Aesar. A fluorometric aldehyde assay kit (MAK141) was obtained from Sigma-Aldrich. DI water (~ 18.2 MΩ•cm) was produced by a Synergy system from Millipore. All reagents were received and used without further purification.

Regenerated cellulose dialysis tubing (molecular weight cutoff (MWCO) 3.5 kDa) was from Fischer Scientific.

104

105

106

107

108

109

110

111

112

113

114

115

116

117

118

119

120

121

122

123

124

125

126

General procedure for amide formation between 1, 3, 4, 6-tetra-O-acetyl-D-glucosamine (acetyl-GlcN) and polysaccharides CMD, alginate, or CMC. The starting polysaccharide was first dissolved in DI water at room temperature (RT) with magnetic stirring. Specifically: CMDNa (1.0 g, 1.2 mmol -COONa) was dissolved in 10 mL DI water, alginic acid sodium salt (0.5 g, 2.5 mmol -COONa) was dissolved in 50 mL DI water, and CMCNa (0.5 g, 1.8 mmol -COONa) was dissolved in 50 mL DI water. Then DMTMM (0.5 g, 1.8 mmol, 1.5 equiv per -COONa for CMDNa; 0.875 g, 3.2 mmol, 1.3 equiv per -COONa for alginic acid sodium salt; or 0.974 g, 3.5 mmol, 1.9 equiv per -COONa for CMCNa) was added to each solution. After 3 h stirring, 1, 3, 4, 6-tetra-O-acetyl-D-glucosamine (1.38 g, 3.6 mmol, 2.9 equiv per -COONa for CMDNa; 2.42 g, 6.3 mmol, 2.5 equiv per -COONa for alginic acid sodium salt; or 2.7 g, 7.0 mmol, 3.8 equiv per -COONa for CMCNa) was added and pH was adjusted to 7.5 using saturated aq. NaHCO₃. The solution was stirred at RT for another 24 h. Then the reaction mixture was transferred to a dialysis tube (cutoff 3.5 kDa) and dialyzed against 0.1 M NaCl for 2 d, then against DI water for 3 d. Solutions were concentrated by freeze drying to afford the products as white, fibrous materials. General procedure for amide formation between D-(+)-glucosamine (GlcN) or D-(+)galactosamine (GalN) and CMD, alginate, or CMC. The starting polysaccharide was first dissolved in DI water at a certain temperature (RT, 37 °C, or 50 °C) under magnetic stirring. Specifically: CMDNa (1.0 g, 1.2 mmol -COONa) was dissolved in 10 mL DI water, alginic acid sodium salt (0.5 g, 2.5 mmol -COONa) was dissolved in 50 mL DI water, and CMCNa (0.5 g, 1.8 mmol -COONa) was dissolved in 50 mL DI water. Then DMTMM (0.5 g, 1.8 mmol, 1.5 equiv per -COONa for CMDNa; 1.17 g, 4.2 mmol, 1.7 equiv per -COONa for alginic acid sodium salt; or

0.974 g, 3.5 mmol, 1.9 equiv per -COONa for CMCNa) was added to the solution. After 3 h stirring at the desired temperature (RT, 37 °C, or 50 °C), D-(+)-glucosamine or D-(+)-galactosamine hydrochloride (0.8 g, 3.7 mmol, 3.0 equiv per -COONa for CMDNa; 3.23 g, 15.0 mmol, 6.0 equiv per -COONa for alginic acid sodium salt; or 1.52 g, 7.0 mmol, 3.8 equiv per -COONa for CMCNa) was added and the pH was then adjusted to 7.5 using saturated aq. NaHCO₃ or dilute aq. NaOH. The solution was stirred for (24 h or 48 h) at the desired temperature (RT, 37 °C, or 50 °C), then the reaction mixture was transferred to a dialysis tube (cutoff 3.5 kDa) and dialyzed against 0.1 M NaCl for 2 d, then against DI water for 3 d. The products were obtained by freeze drying to afford white, fibrous materials. Reaction duration was controlled at 24 or 48 h, and reaction temperature was controlled at RT, 37 °C, or 47 °C to determine the impact upon conversion. Yields: alginate-GlcN, 0.32 g, 60 %. General procedure for silver mirror reaction and hydrogel formation. Silver oxide (0.2 g, Ag₂O) was dissolved in 2 mL dilute aq NH₄OH (10% w/v) in a test tube. Polysaccharide (30 mg) was dissolved in 2 mL DI water in a vial, and the polysaccharide solution was added to the test tube which was then shaken by hand. Finally, the test tube was placed into a 70 °C water bath for 30 min. For hydrogel formation, 1.0 g poly(ethyleneimine) and 0.05 g multi-reducing-end alginate were each dissolved in 1 mL DI water in separate 20 mL vials, and the two solutions were combined and left at room temperature for 24 h. Quantitative analysis of aldehyde concentration in starting polysaccharides and product multi-reducing-end polysaccharides using a fluorometric method. A fluorometric aldehyde assay kit was used. The standard curve of emission fluorometric intensity vs. concentration of aldehydes was obtained by following the procedure from the kit instructions. Each polysaccharide

127

128

129

130

131

132

133

134

135

136

137

138

139

140

141

142

143

144

145

146

147

148

sample was dissolved in DI water at 10 mg/mL. Aliquots (50 µL) of these solutions were added to wells of a 96-well plate. All samples were tested in duplicate; standard deviations of the results were below 5%. The fluorescence excitation wavelength was 365 nm while the emission wavelength was 435 nm.

Characterization. ¹H and ¹³C NMR spectra were obtained on a Bruker Avance II 500 MHz spectrometer in deuterated water (D₂O) at room temperature, using 128 scans for ¹H NMR and

150

151

152

153

154

155

156

157

158

159

160

161

162

163

164

165

166

167

168

169

170

171

10,000 scans for ¹³C NMR spectra. ¹H NMR spectra were referenced to D₂O (4.79 ppm). ¹³C NMR spectra were referenced to 3-(trimethylsilyl) propionic-2,2,3,3-d4 acid, sodium salt (0 ppm). Diffusion ordered spectroscopy (DOSY) was performed on a Bruker Avance III 400 MHz spectrometer equipped with a Diff50 diffusion probe. DOSY experiments were run with a 1 ms gradient pulse duration, 20 ms diffusion encoding time, and 16 steps of the gradient strength, with 64 scans per step. A fluorometric method was used to quantify aldehyde concentration of polysaccharide samples, employing a fluorometric aldehyde assay kit from Sigma and a microplate reader (TECAN infinite M200 PRO) to read fluorescence. The open chain aldehyde form of each polysaccharide reducing end will react with a fluorescent dye from the assay kit and emit strong fluorescence at 435 nm wavelength with excitation wavelength of 365 nm. Size exclusion chromatography (SEC) was performed using instrumentation consisting of Wyatt Technologies DAWN 8 light scattering and Optilab refractive index detectors. One Shodex Ohpak LB-806M column heated to 40 °C was used with a mobile phase consisting of DI water/100 mM NaNO₃ as the eluent and a Shimadzu LC-40D with pump operating at 1.0 mL/min. DS(CM) of CMD and CMC, G/M ratio of alginate, yields, and aldehyde concentrations were calculated according to the following equations:

DS(CM) of CMC, based on the ¹H NMR spectrum of the hydrolysis product:

$$DS(CM) = \frac{I(2 \text{ protons of CM side chain})/2}{I(H2 - H6 \text{ from cellulose backbone})/6}$$
(1)

- 173 The hydrolysis procedure and NMR assignments were based on the previous literature³⁶. Protons
- of CM side chain (-OCH₂COO⁻) are from 4.15 4.55 ppm. Protons H2 H6 from cellulose
- backbone are from 3.15 4.10 ppm.
- 176 DS(CM) of CMD, based on the ¹H NMR spectrum of CMD:

$$\frac{2 \times DS(carboxymethyl group)}{1} = \frac{I(a)}{I(H1)}$$
 (2)

- 177 I(a) refers to the integral of the CM methylene resonance in the ¹H NMR spectrum of CMD (**Fig**
- 178 S2). I(H1) is the integral of the CMD H1 resonance (Fig. S2).
- 179 G/M ratio of alginic acid sodium salt, based on the ¹H NMR spectrum of partial hydrolyzed
- 180 alginate:

$$\frac{M}{G} = \frac{I(B) + I(C) - I(A)}{I(A)} = 1.9$$
(3)

- The partial hydrolysis and NMR analysis methods were based on the previous literature³⁷. I(A),
- 182 I(B) and I(C) refer to the integrals of peaks A, B and C in the ¹H NMR spectrum of partially
- hydrolyzed alginate (Fig. S3).
- 184 Yields of products:

$$\%Yield = \frac{\text{moles of product}}{\text{moles of reactant}} \tag{4}$$

- Product aldehyde concentration (the equation is from calibration curve of aldehyde concentration
- vs. fluorescence intensity **Fig. S12**):

Aldehyde concentration =
$$\frac{\text{Fluoroscence intensity} - 26843}{117.4}$$
 (5)

Determination of the DS(GlcN) of alginate-GlcN (based on **Fig. 4**):

$$\frac{2 \times DS(GlcN)}{1} = \frac{I(a\alpha) + I(d\alpha + d\beta + e\beta)}{I(G1) \times (1 + M/G \text{ ratio})}$$
(6)

Calculation of the aldehyde concentration of alginate-GlcN based on its

$$DS(GleN)$$
: (7)

$$c(GlcN) = \frac{m \times DS(GlcN)}{M(AlginateGlcN) \times V}$$

- $\frac{m}{v}$ is 10 mg/mL. c(GlcN) is the concentration of the appended glucosamine (also the aldehyde
- concentration). DS(GlcN) is the DS of GlcN of alginate-GlcN. M(AlginateGlcN) is the molecular
- weight per AGU of the alginate-GlcN sample analyzed by NMR spectroscopy.

191

- 192 Determination of alginate-GlcN estimated real DS(GlcN) using measured aldehyde concentrations
- and NMR value 0.17 (equivalent equation used for alginate-GalN DS(GalN)):

(8)

$$DS(GlcN) = 0.17 \times \frac{A(AlginateGlcN)}{49.51 \,\mu\text{M}}$$

- 194 A is aldehyde concentration in **Table 1**. The numbers 0.17 and 49.51 μM are DS(GlcN) and A of
- the alginate-GlcN sample analyzed by NMR. The difference of molecular weight per AGU
- between different alginate-GlcN samples was neglected.

- 198 Determination of CMD-GlcN estimated real DS(GlcN) using aldehyde concentrations and NMR
- value 0.17 (same equation for CMD-GlcN DS(GalN)):

$$DS(GlcN) = 0.17 \times \frac{A(CMDGlcN)}{49.51 \,\mu\text{M}} \times \frac{M(CMD)}{M(AlginateGlcN)}$$
(9)

A is aldehyde concentration in **Table 1**. The 0.17, 49.51 µM and M(AlginateGlcN) are DS(GlcN),

A and molecular weight per AGU of the alginate-GlcN sample analyzed by NMR. The difference

of molecular weight per CMD-GlcN AGU compared to CMD AGU was neglected. The difference

of molecular weight per alginate-GlcN AGU caused by different DS(GlcN) was neglected.

Determination of CMC-GlcN estimated real DS(GlcN) using aldehyde concentrations and NMR

value 0.17 (same equation for CMC-GlcN DS(GalN)):

(10)

$$DS(GlcN) = 0.17 \times \frac{A(CMCGlcN)}{49.51 \,\mu\text{M}} \times \frac{M(CMC)}{M(AlginateGlcN)}$$

A is aldehyde concentration in **Table 1**. The 0.17, 49.51 μM and M(AlginateGlcN) are DS(GlcN), A and molecular weight per AGU of the alginate-GlcN sample analyzed by NMR. The difference of molecular weight per CMC-GlcN AGU compared to CMC AGU was neglected. The difference of molecular weight per alginate-GlcN AGU caused by different DS(GlcN) was neglected.

RESULTS AND DISCUSSION

Reactions of 1, 3, 4, 6-tetra-*O*-acetyl-D-glucosamine (acetyl-GlcN) with polysaccharides. We selected acetyl-GlcN as our initial substrate for amide formation, and selected three commercial carboxyl-containing polysaccharides, CMD, CMC, and alginate (Scheme 1). Acetyl-GlcN was useful for initial experiments because its acetyl groups have ¹H NMR resonances upfield of the typical polysaccharide backbone region (around 2 ppm), and likewise ¹³C NMR resonances upfield (around 20 ppm) of those typical for polysaccharides. These resonances are sharp, readily

distinguished, and (for protons) readily integrated in comparison with the more downfield backbone resonances of the starting polysaccharides.

218

219

220

221

222

223

224

225

226

227

228

229

230

231

232

233

234

235

236

237

238

239

We chose to initiate reaction of acetyl-GlcN with CMD using 4-(4,6-dimethoxy-1,3,5-triazin-2-yl)-4-methylmorpholinium chloride (DMTMM) because it is an efficient, widely used coupling agent for amide formation.^{38–40} The reaction (RT, 24 h) afforded a water-soluble product that could be purified by dialysis and isolated by freeze-drying. In its ¹H NMR spectrum (Fig. 1), the sharp resonance at 2.16 ppm and the small one at 2.11 ppm were assigned to acetyl groups from the appended monosaccharide acetyl-GlcN. It is noted that some of the acetyl resonances of these derivatives appeared to be weaker than those of the starting monosaccharide (Fig. S4). There are two possible reasons for the weaker acetyl signal; one is that the DS of acetyl-GlcN on the CMD is low, the other is there may be partial acetyl hydrolysis during the alkaline amide formation reaction conditions. De-acylation of polysaccharide and carbohydrate esters under alkaline conditions is rapid as has been previously observed, including in work by our group. 41,42 These results were supported by ¹³C NMR spectroscopy (Fig. 2), where the resonance at 23 ppm was assigned to the acetyl methyls from the appended monosaccharide acetyl-GlcN. Successful amide formation between the acetyl-GlcN amine and CMD carboxyls was further confirmed by diffusion-ordered NMR spectroscopy (DOSY) experiments (Fig. S14), 43,44 which revealed that all resonances associated with the polymer chain, including those arising from both acetyl-GlcN and CMD moieties, exhibited identical self-diffusion coefficients (6.1 \times 10⁻¹¹ \pm 1 \times 10⁻¹² m² s⁻¹). This strongly supported the conclusion that acetyl-GlcN and CMD were covalently attached to one another.

Scheme 1. Amide-forming reactions of acetyl-GlcN with polysaccharides. **A.** CMD and acetyl-GlcN. **B.** CMC and acetyl-GlcN. **C.** Alginate and acetyl-GlcN. Note that positions of carboxymethyl substitution in this and other schemes and figures are not meant to denote regioselective substitution but are displayed in this way only for simplicity and clarity.

We were also able to demonstrate successful amide formation between acetyl-GlcN and CMC, as well as with alginate, a natural polysaccharide produced by kelp and bacteria. Each alginate monosaccharide is a uronic acid ($1\rightarrow4$ -linked β -D-mannuronic acid (M) or $1\rightarrow4$ -linked α -L-guluronic acid (G)). In the 1 H NMR spectrum of the purified amide resulting from coupling CMC and acetyl GlcN (**Fig. S6**), the resonance at 2.1 ppm is assigned to the acetyl groups of the appended monosaccharide. Both 1 H NMR and 13 C NMR spectra of the purified alginate-acetyl

GlcN product also fully supported successful amide formation, and typical resonances related to M and G could be identified in the product's ¹H NMR spectrum; they were assigned based on literature values. ⁴⁵ The ¹H NMR spectrum of alginate-acetyl GlcN also displayed a prominent, broad peak at ca. 2.1 ppm which we assigned to the acetyl methyls of the attached monosaccharide (**Fig. 3**). Methyl carbons of the acetyl groups (23 ppm) were also observed in the ¹³C NMR spectra of alginate-acetyl GlcN (**Fig. S7**). Covalent attachment of acetylated GlcN to CMC and alginate, rather than simple mixing, was strongly supported by the similar diffusion coefficients (DOSY) of resonances arising from acetyl GlcN and the backbone regions of CMC and alginate, respectively (**Fig. S15 and S16**).



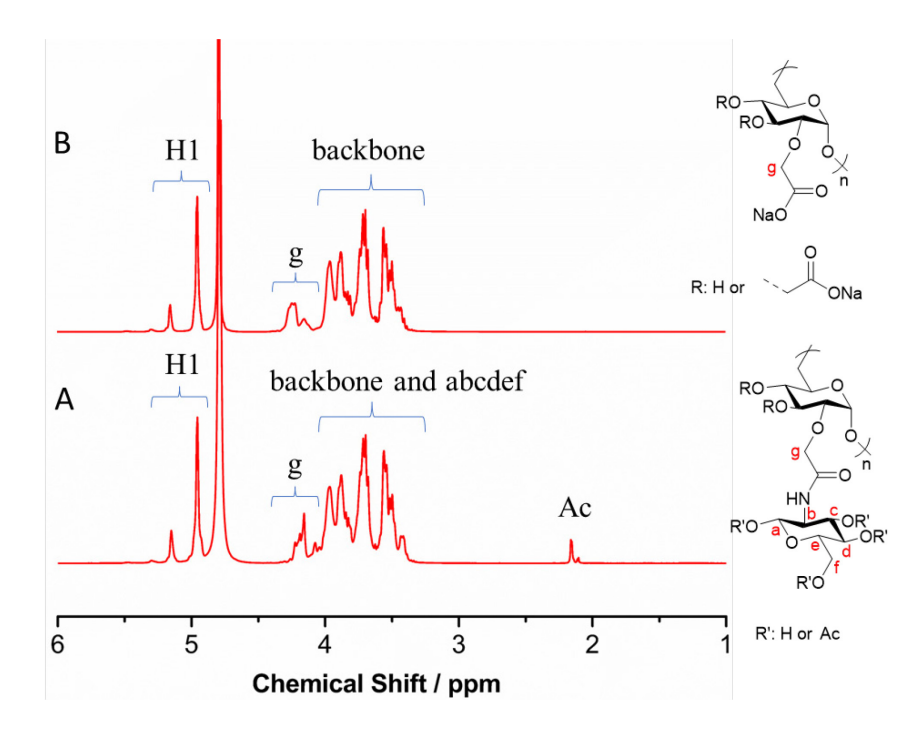
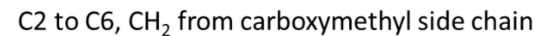


Figure 1. ¹H NMR spectra. A. CMD-acetyl GlcN, B. CMD.



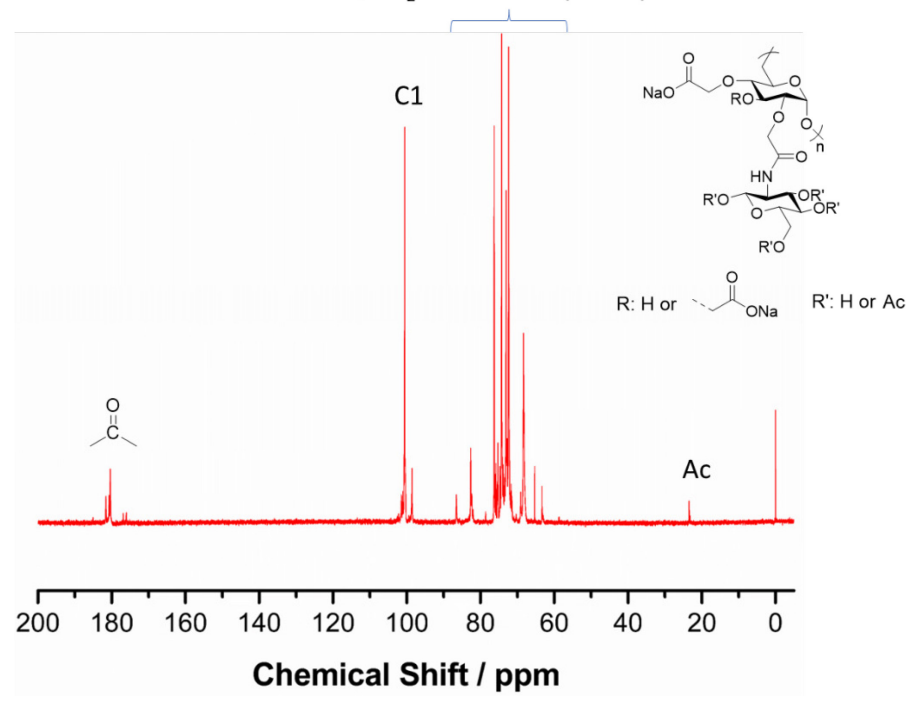


Figure 2. ¹³C NMR spectrum of CMD-acetyl GlcN.

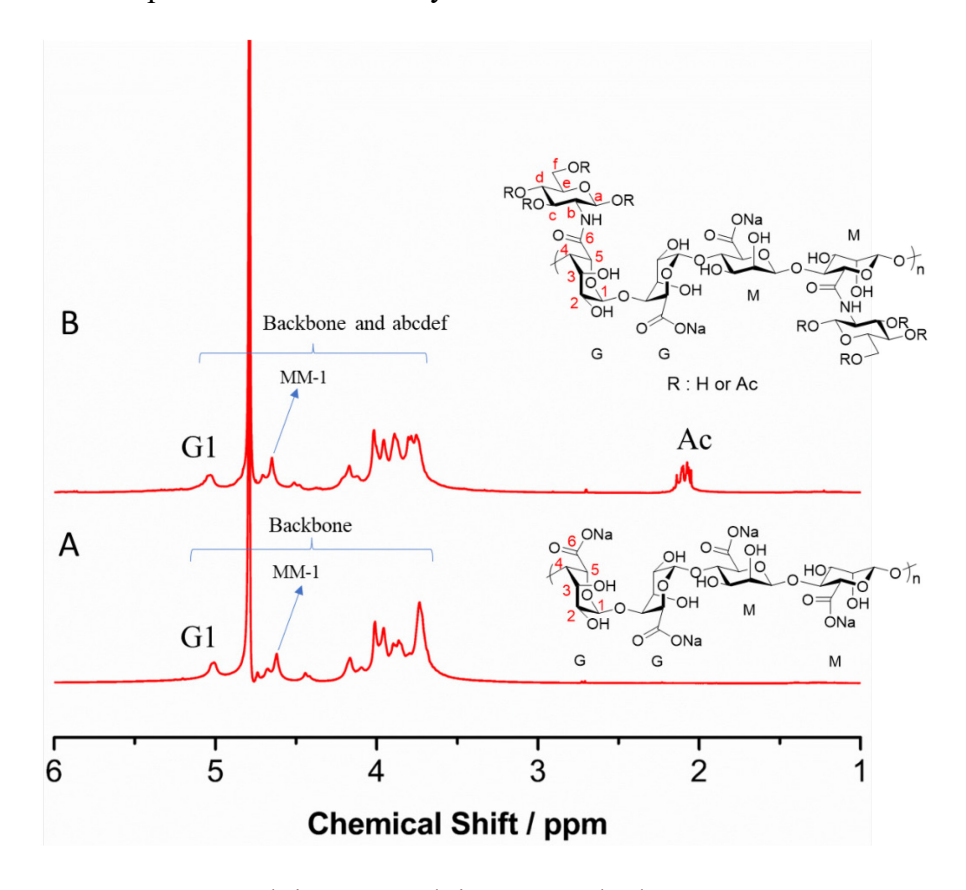


Figure 3. ¹H NMR spectra. A. Alginate, B. Alginate-acetyl GlcN.

Reactions of D-glucosamine (GlcN) and D-galactosamine (GalN) with polysaccharides.

Having shown successful amide formation between 2-amino-2-deoxymonosaccharide esters and polysaccharide carboxyl groups by using acetyl-GlcN with its ¹H NMR-prominent ester groups, we examined amide formation between unsubstituted GlcN and GalN and carboxyl-containing polysaccharides (CMD, CMC, and alginates, **Scheme 2**). In the process, we explored the impact of key reaction parameters upon conversion. Lacking the obvious ¹H NMR handles of acetyl methyls, we quantified the reducing ends added upon reaction with amino sugars to form MREPs by a fluorometric method which is commonly used to quantify aldehydes. ^{46,47}

Scheme 2. Reactions of 2-amino-2-deoxymonosaccharides with carboxyl-containing polysaccharides (illustrated using GlcN). Reactions of GlcN with **A.** CMD, **B.** CMC, **C.** Alginate.

Despite the similar structural features of the aminomonosaccharides and polysaccharides, and the absence of obvious reporter groups in GlcN or GalN (i.e., acetyl groups), some evidence for successful amide formation could be found in the NMR spectra of alginate-GlcN. In the ¹H NMR spectrum (Fig. 4), a new resonance was observed at 3.5 ppm, and we speculated that this new resonance was from specific protons of the newly appended monosaccharide. Heteronuclear Single-Quantum Correlation Spectroscopy (HSQC) (Fig. S10) of alginate-GlcN was employed to confirm this hypothesis. We observed correlations of the new ¹H resonance at 3.5 ppm with two ¹³C resonances at 73 and 79 ppm. We examined the simple but structurally similar compound, GlcNAc, to help support the NMR assignments of product resonances (Fig. S8). In the HSQC spectrum of GlcNAc (Fig. S11), its ¹H resonance at ~3.5 ppm was correlated to ¹³C resonances at 73 and 79 ppm, which could be assigned to C4 and C5 of the β-anomer of GlcN. 48 By analogy, we assigned the new ¹H resonance at 3.5 ppm to the C4 and C5 protons of the β-anomer of the newly attached glucosamine, shown in Fig. 4. Since the anomeric position of the attached aminomonosaccharide is unsubstituted, both anomers are observed, with the equatorial anomer predominant. The DS(GlcN) was calculated based on the integral ratio of the new resonances at 3.5 and 5.2 ppm to the resonances of G1 at 5.0 ppm. Based on integration of the ¹H NMR spectrum (Fig. 4) and equation (6), DS(GlcN) is calculated to be 0.17. We observed that H2-C2 correlation of the appended GlcN from the alginate-GlcN product (Fig. S10) matched those of the GlcNAc model (Fig. S11) well, supporting the hypothesis that GlcN was linked to alginate via an amide bond. Additional evidence of successful linkage was also found in the ¹³C NMR spectra, shown in Fig. 5. The C1, C2 and C6 resonances of the appended monosaccharide were clearly observed in the ¹³C NMR spectrum of the final product alginate-GlcN. In addition, we compared the product ¹H NMR spectrum with that of GlcN itself (**Fig. S9**). Resonances at 2.5 ppm (from H2 of GlcN)

279

280

281

282

283

284

285

286

287

288

289

290

291

292

293

294

295

296

297

298

299

300

were absent in the ¹H NMR spectrum of the amide alginate-GlcN, indicating that it contained no free monosaccharide within ¹H NMR detection limits.⁴⁹ It was also of interest to examine the loss of DP that occurred during the conjugation reaction, in the presence of a base. Size exclusion chromatography of the GlcN adducts of alginate, carboxymethyl dextran, and carboxymethyl cellulose showed moderate loss of DP, ranging between 25-60%. No attempt was made within the bounds of the current study to maximize conditions for preservation of DP.

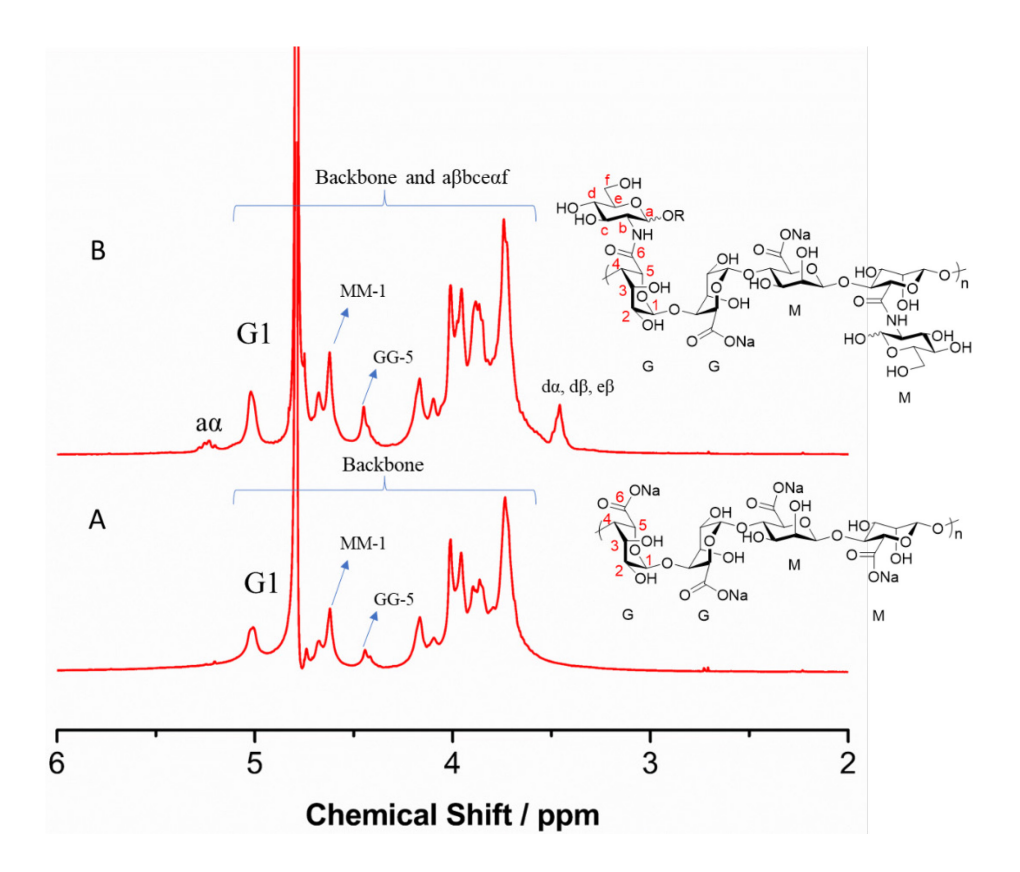


Figure 4. ¹H NMR spectra. A. Alginate, B. Alginate-GlcN.

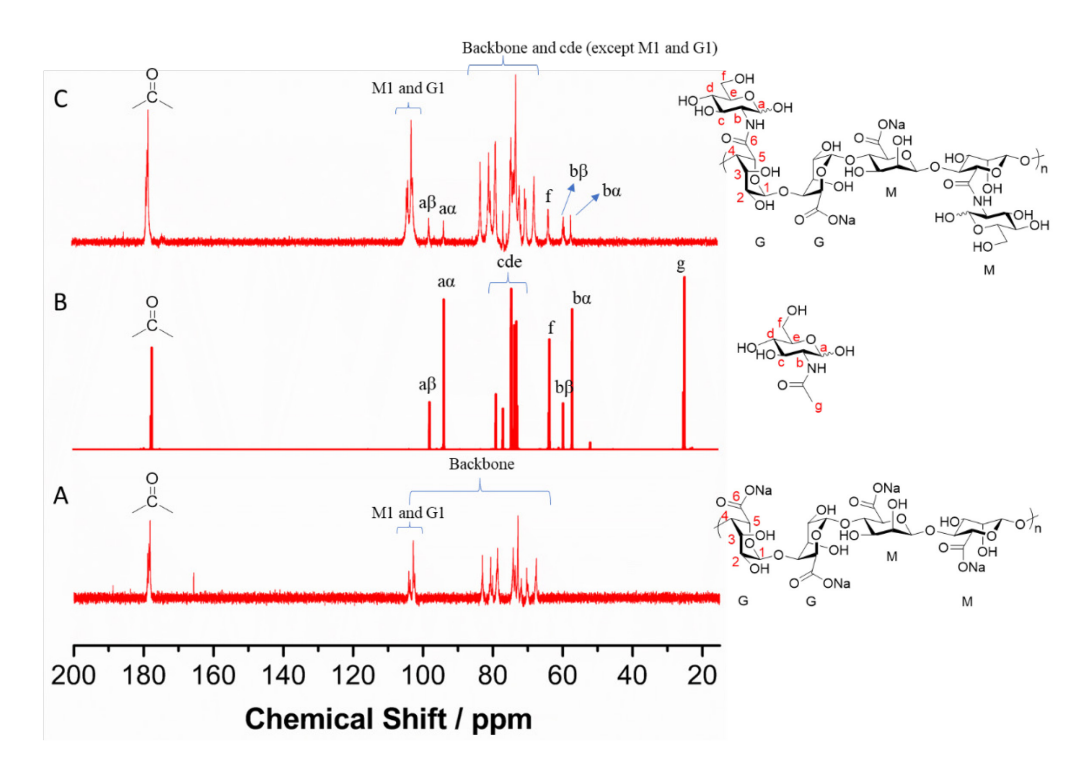


Figure 5. ¹³C NMR spectra. A. Alginate, B. GlcNAc, C. Alginate-GlcN.

Study of the relationship between reaction parameters and conversion using a fluorometric method. To study the relationship between conversion and parameters such as reaction temperature and time, a fluorometric method was used employing a microplate reader. Amide conversion was directly proportional to the aldehyde concentration of the MREP amide products. Aldehyde concentration could be measured by conversion of the aldehydes to fluorescent adducts, which fluoresce at 435 nm upon 365 nm excitation. By measuring the emission fluorescence intensity of these adducts at 435 nm and comparing with a standard curve of aldehyde concentration vs. fluorescence intensity (Fig. S12), the aldehyde concentration of the samples could be quantified. Reaction parameters and the resulting aldehyde concentrations are shown in Table 1; each MREP had fluorescence intensity higher than that of the relevant starting polysaccharide, as expected and further supporting successful introduction of reducing ends by amide formation with the 2-amino-2-deoxymonosaccharides. Product aldehyde concentration seemed to be insensitive to changes in aminomonosaccharide type, reaction time, or reaction temperature. However, by switching the added base (used to neutralize acid from GlcN or GalN, supplied as HCl salts) from sodium bicarbonate to sodium hydroxide, conversion was improved. We hypothesize that this was due to reaction of the NaHCO₃ neutralization by-product CO₂ with the monosaccharide amine groups, forming carbamic acids and thus interfering with amide formation.⁵⁰ This side reaction was circumvented by using NaOH as base. As stated before, the DS(GlcN) of Alg-GlcN was calculated to be 0.17 based on integration of the ¹H NMR spectrum (**Fig. 4**). Alg-GlcN with DS(GlcN) 0.17 corresponds to entry 24 in Table 1, where NaOH was used to neutralize the HCl from GlcN. Converting the DS to aldehyde concentration based on equation (7), the aldehyde concentration should be 7597 µM instead of the measured 49.51 µM (**Table 1**). The reason for this large difference is that not all the reducing ends

314

315

316

317

318

319

320

321

322

323

324

325

326

327

328

329

330

331

332

333

334

335

of the appended monosaccharide are converted to the fluorescent adducts, due to the nature of the reducing end, which is in equilibrium between a ring-closed hemiacetal and an open-chain aldehyde form. The estimated DS ("DS") of the multi-reducing end polysaccharides in Table 1 was calculated based on equations (8), (9) and (10).

Table 1. Reaction parameters, aldehyde concentration, and DS (GlcN/GalN) of MREPs.

	PS	Amine	Equiv	DMTMM	Temp.	Time	Base	A	DS
				(eq/CO ₂ -)	(°C)	(h)			
1	CMD	/	/	/	/	/	/	/	
2	CMD	GalN	0.75	0.375	25	24	NaHCO ₃	7.77	0.02
3	CMD	GalN	3.0	1.5	25	24	NaHCO ₃	11.72	0.03
4	CMD	GalN	3.0	1.5	25	48	NaHCO ₃	12.79	0.04
5	CMD	GalN	3.0	1.5	37	48	NaHCO ₃	11.73	0.03
6	CMD	GalN	3.0	1.5	50	48	NaHCO ₃	11.53	0.03
7	CMD	GlcN	3.0	1.5	25	24	NaHCO ₃	11.86	0.03
8	CMD	GlcN	3.0	1.5	25	48	NaHCO ₃	12.38	0.03
9	CMD	GlcN	3.0	1.5	37	48	NaHCO ₃	11.01	0.03
10	CMD	GlcN	3.0	1.5	50	48	NaHCO ₃	11.75	0.03
11	CMD	GlcN	3.0	1.5	25	48	NaOH	16	0.04
12	CMC	/	/	/	/	/	/	/	
13	CMC	GlcN	3.8	1.9	25	48	NaHCO ₃	22.36	0.08
14	CMC	GlcN	3.8	1.9	37	48	NaHCO ₃	22.61	0.08
15	CMC	GalN	3.8	1.9	25	24	NaHCO ₃	22.1	0.08
16	CMC	GalN	3.8	1.9	25	48	NaHCO ₃	22.58	0.08
17	Alg	/	/	/	/	/	/	/	
18	Alg	GlcN	6.0	1.7	25	24	NaHCO ₃	39.31	0.13

19	Alg	GleN	6.0	1.7	25	48	NaHCO ₃	39.82	0.14
20	Alg	GlcN	6.0	1.7	37	48	NaHCO ₃	39.04	0.13
21	Alg	GlcN	6.0	1.7	50	48	NaHCO ₃	39.61	0.14
22	Alg	GlcN	6.0	1.7	25	48	NaOH	48.25	0.17
23	Alg	GalN	6.0	1.7	25	48	NaHCO ₃	39.63	0.14
24	Alg	GlcN	6.0	1.7	37	48	NaOH	49.51	0.17*

PS: starting polysaccharides; Amine: reacting aminosaccharide; Equiv: equivalents aminosaccharide/-COONa; DMTMM: coupling agent used (equiv/-COONa); A: aldehyde concentration (μM) measured by fluorescence. DS: estimated degree of substitution of the appended monosaccharide calculated based on equation (8), (9) and (10)

Silver mirror reaction and hydrogel formation of multi-reducing-end polysaccharides. To provide additional evidence for the successful introduction of reducing ends to polysaccharides, silver mirror reactions were conducted. The silver mirror reaction is a powerful tool to identify aldehyde groups in polysaccharides and other materials, with higher aldehyde concentration affording faster silver mirror reaction. Indeed, after 15 minutes at 70 °C (Fig. 6), a beautiful silver mirror was formed on the surface of the tube for the multi-reducing-end alginate, alginate-GlcN. In comparison, no silver was observed on the surface using unmodified starting alginate, with its far lower reducing end content. Similar results were observed for CMD vs. CMD-GlcN (Fig. S13). In order to demonstrate the potential application of MREPs for making hydrogels, multi-reducing-end alginate solution was mixed with branched poly(ethylene imine) (PEI) solution. Equal volumes of 5 wt% multi-reducing-end alginate solution and 50 wt% branched polyethyleneimine solution in water were mixed, and after 24 h, a hydrogel was formed (Fig. 7). The appended monosaccharide is in equilibrium between a ring-closed hemiacetal and an open-

^{*} This value was calculated by ¹H NMR spectrum (Fig. 4).

chain aldehyde form. The excess amine groups of the branched poly(ethyleneimine) react with aldehydes of the appended monosaccharides to form Schiff base bonds, and this reaction pushes the equilibrium to the open-chain aldehyde form. In a control experiment, equal volumes of 5 wt% alginate solution and 50 wt% branched poly(ethyleneimine) solution in water were mixed at room temperature. No hydrogel was observed after 24 h. In fact, these mixed control solutions could still flow after one week. To exclude the possibility that Alg-GlcN/PEI gelation was caused by the slight pH difference between alginate and alginate-GlcN solution, another control experiment was conducted. The alginate solution was adjusted using acetic acid to the same pH as the alginate-GlcN solution. Even after the pH adjustment, no gelation of the alginate/branched PEI mixture was observed after 24 h. We are actively exploring methods to facilitate and accelerate this gelation process.





Figure 6. Silver mirror reaction of alginate (left in each photo) and alginate-GlcN (right in each photo).



Figure 7. Hydrogel formation by mixing alginate-GlcN solution (left) and branched poly(ethylene imine) solution (middle) to form the hydrogel depicted on the (right).

CONCLUSIONS

378

379

380

381

382

383

384

385

386

387

388

389

390

391

392

393

394

395

396

397

In this work, a new family of polysaccharides termed multi-reducing-end polysaccharides (MREP) has been prepared using the synthetic strategy of reacting polysaccharide carboxylic acid groups with the amines of 2-amino-2-deoxymonosaccharides to form amide linkages, employing DMTMM as coupling agent. Reactions of carboxymethyl dextran (CMD), carboxymethyl cellulose (CMC), or alginate with glucosamine (GlcN) or galactosamine (GalN) afforded wellcharacterized products in which the 2-amino-2-deoxymonosaccharide was attached to the polysaccharide through an amide linkage. As a result, each amide-appended monosaccharide had an intact anomeric position, that is to say its reducing end. Multiple reactive aldehyde groups were thus appended to each polysaccharide molecule, with no loss of cyclic monosaccharide structure in the polysaccharide, and thus no introduction of undesired flexibility or chemical instability. NMR techniques were used to indicate successful linkage to polysaccharides through the 2-amine groups of the monosaccharides. A fluorometric method was used to confirm aldehyde concentrations in cases where interpretation of the ¹H NMR spectrum and its integration were difficult, due to resonance overlaps. These aldehyde concentration results enabled us to identify the insensitivity of reaction conversion to time and temperature within the ranges studied, the similar reactivities of GlcN and GalN, and the superior performance of NaOH vs. NaHCO₃ base. The silver mirror reaction provided important qualitative, visual evidence for successful MREP synthesis. The formation of a hydrogel upon reaction of MREP with branched poly(ethylene imine) illustrated one example of the widespread application potential of these MREPs. Overall, this work is promising for decorating many types of polysaccharides, including those with natural carboxylic acid content (those containing uronic acid monosaccharides) and those with carboxylcontaining substituents (such as carboxymethyl or ω-carboxyalkanoyl-substituted polysaccharide derivatives) with amine-containing monosaccharides to afford multi-reducing-end polysaccharides. MREPs have promise for many other potential applications, such as conjugating with proteins or drugs to create prodrugs for targeted or slow-release therapeutics or making allpolysaccharide hydrogels with chitosan through dynamic Schiff base bonds. Reducing such concepts to practice is currently underway in our laboratory.

410

411

412

398

399

400

401

402

403

404

405

406

407

408

409

ASSOCIATED CONTENT

Supporting Information

- The following files are available free of charge.
- 414 ¹H NMR spectra for hydrolyzed carboxymethyl cellulose, carboxymethyl dextran, partially
- hydrolyzed alginate, 1, 3, 4, 6-tetra-O-acetyl-D-glucosamine (acetyl-GlcN), CMC-acetyl GlcN,
- N-acetylglucosamine and neutralized D-2-amino-2-deoxyglucose. ¹³C NMR spectra for 1, 3, 4, 6-
- 417 tetra-O-acetyl-D-glucosamine (acetyl-GlcN), Alginate and alginate-acetyl GlcN. HSQC NMR
- 418 spectra for Alg-GlcN and GlcNAcCMD. ¹H DOSY spectra for CMD-acetyl GlcN, CMC-acetyl
- 419 GlcN and Alg-acetyl GlcN. Silver mirror reaction pictures of CMD and CMD-GlcN. Table for
- 420 the reaction parameters and aldehyde concentration of MREPs using fluorometric method (PDF).

- 421
- 422 AUTHOR INFORMATION
- 423 Corresponding Author
- 424 Kevin J. Edgar -- Department of Sustainable Biomaterials and Macromolecules Innovation
- 425 Institute, Virginia Tech, Blacksburg, VA 24061, United States; orcid.org/0000-0002-9459-9477;
- 426 Email: kjedgar@vt.edu
- 427 Authors
- 428 Zhenghao Zhai‡ -- Macromolecules Innovation Institute, Virginia Tech, Blacksburg, VA 24061,
- 429 United States
- 430 Yang Zhou‡ -- Department of Sustainable Biomaterials, Virginia Tech, Blacksburg, VA 24061,
- 431 *United States*
- 432 Andrew G. Korovich -- Department of Chemistry and Macromolecules Innovation Institute,
- 433 Virginia Tech, Blacksburg, VA 24061, United States
- 434 Brady A. Hall GlycoMIP, Fralin Life Sciences Institute, Virginia Tech, Blacksburg, VA 24061,
- 435 United States
- 436 Hu Young Yoon -- Macromolecules Innovation Institute, Virginia Tech, Blacksburg, VA 24061,
- 437 *United States*
- 438 Yimin Yao -- Department of Chemical Engineering and Macromolecules Innovation Institute,
- 439 Virginia Tech, Blacksburg, VA 24061, United States
- Junchen Zhang -- Department of Biological Sciences, Virginia Tech, Blacksburg, VA 24061,
- 441 United States
- 442 Michael J. Bortner -- Department of Chemical Engineering and Macromolecules Innovation
- 443 Institute, Virginia Tech, Blacksburg, VA 24061, United States

444	Maren Roman Department of Sustainable Biomaterials and Macromolecules Innovation
445	Institute, Virginia Tech, Blacksburg, VA 24061, United States
446	Louis A. Madsen Department of Chemistry and Macromolecules Innovation Institute, Virginia
447	Tech, Blacksburg, VA 24061, United States
448	Author Contributions
449	Z. Z., and Y. Z. designed and executed the research. Z. Z. and Y. Z. performed synthesis,
450	characterization, and application experiments and collected the data. A. G. K. and L. A. M.
451	provided the DOSY experiment and data analysis. B. H., H. Y. Y. and M. R. helped with the
452	molecular weight characterization of the starting materials. Y. Y. and M. J. B. helped with the
453	hydrogel formation experiment. J. Z. helped with the MREPs synthesis. Z. Z., Y. Z. and K. J. E.
454	wrote the manuscript. All authors have given approval to the final version of the manuscript.
455	‡These authors contributed equally.
456	
457	Notes
458	The authors declare no competing financial interest.
459	
460	ACKNOWLEDGMENTS
461	This work was supported by GlycoMIP, a National Science Foundation Materials Innovation
462	Platform funded through Cooperative Agreement DMR-1933525. MR acknowledges support by
463	the Virginia Agricultural Experiment Station and the Hatch Multistate Program of the National
464	Institute of Food and Agriculture, U.S. Department of Agriculture.
465	We thank the Virginia Tech Institute for Critical Technology and Applied Science, the
466	Macromolecules Innovation Institute for partial support of this work. We thank Dr. Jiang, Dr.

- 467 Gilbert and Dr. Cline's group for providing the microplate reader. We are grateful for the U. S.
- Department of Agriculture (NIFA) for partial support of this work through grant 2020-67021-
- 469 31379 (ZZ). We thank Dr. Murthy Shanaiah for guidance about NMR experiments.

471 **ABBREVIATIONS**

- 472 MREPs, multi-reducing-end polysaccharides; CMC, carboxymethyl cellulose; CMD,
- 473 carboxymethyl dextran; DMTMM, 4-(4,6-dimethoxy-1,3,5-triazin-2-yl)-4-methylmorpholinium
- 474 chloride; GlcN, glucosamine; GalN, galactosamine; HSQC, Heteronuclear Single-Quantum
- 475 Correlation Spectroscopy; DOSY, diffusion-ordered NMR spectroscopy.

476

477

REFERENCES

- 478 (1) Deng, Y.; Li, J.; Sun, C.; Chi, H.; Luo, D.; Wang, R.; Qiu, H.; Zhang, Y.; Wu, M.; Zhang, 479 X.; Huang, X.; Xie, L.; Qin, C. Rational Development of a Polysaccharide–Protein-Conjugated Nanoparticle Vaccine Against SARS-CoV-2 Variants and Streptococcus 481 Pneumoniae. *Advanced Materials* **2022**, *34* (21). https://doi.org/10.1002/adma.202200443.
- 482 (2) Shapiro, E. D.; Berg, A. T.; Austrian, R.; Schroeder, D.; Parcells, V.; Margolis, A.; Adair, R. K.; Clemens, J. D. The Protective Efficacy of Polyvalent Pneumococcal Polysaccharide Vaccine. New England Journal of Medicine 1991, 325 (21), 1453–1460. https://doi.org/10.1056/NEJM199111213252101.
- 486 (3) Dong, Y.; Mosquera-Giraldo, L. I.; Troutman, J.; Skogstad, B.; Taylor, L. S.; Edgar, K. J. Amphiphilic Hydroxyalkyl Cellulose Derivatives for Amorphous Solid Dispersion Prepared by Olefin Cross-Metathesis. *Polym Chem* **2016**, 7 (30), 4953–4963. https://doi.org/10.1039/c6py00960c.
- 490 (4) Winslow, C. J.; Nichols, B. L. B.; Novo, D. C.; Mosquera-Giraldo, L. I.; Taylor, L. S.;
 491 Edgar, K. J.; Neilson, A. P. Cellulose-Based Amorphous Solid Dispersions Enhance
 492 Rifapentine Delivery Characteristics in Vitro. *Carbohydr Polym* 2018, *182*, 149–158.
 493 https://doi.org/10.1016/j.carbpol.2017.11.024.
- 494 (5) Zhou, Y.; Zhai, Z.; Yao, Y.; Stant, J. C.; Landrum, S. L.; Bortner, M. J.; Frazier, C. E.; Edgar, K. J. Oxidized Hydroxypropyl Cellulose/Carboxymethyl Chitosan Hydrogels Permit PH-Responsive, Targeted Drug Release. *Carbohydr Polym* **2023**, *300*, 120213. https://doi.org/https://doi.org/10.1016/j.carbpol.2022.120213.

- 498 (6) Tchobanian, A.; van Oosterwyck, H.; Fardim, P. Polysaccharides for Tissue Engineering: Current Landscape and Future Prospects. *Carbohydrate Polymers*. Elsevier Ltd February 1, 2019, pp 601–625. https://doi.org/10.1016/j.carbpol.2018.10.039.
- 501 (7) Khan, F.; Ahmad, S. R. Polysaccharides and Their Derivatives for Versatile Tissue Engineering Application. *Macromolecular Bioscience*. April 2013, pp 395–421. https://doi.org/10.1002/mabi.201200409.
- 504 (8) Zhou, Y.; Petrova, S. P.; Edgar, K. J. Chemical Synthesis of Polysaccharide—Protein and Polysaccharide—Peptide Conjugates: A Review. *Carbohydr Polym* **2021**, 274. https://doi.org/10.1016/j.carbpol.2021.118662.
- 507 (9) Zhou, Y.; Edgar, K. J. Regioselective Synthesis of Polysaccharide–Amino Acid Ester Conjugates. *Carbohydr Polym* **2022**, 277. https://doi.org/10.1016/j.carbpol.2021.118886.
- 509 (10) Cumpstey, I. Chemical Modification of Polysaccharides. *ISRN Org Chem* **2013**, *2013*, 510 417672. https://doi.org/10.1155/2013/417672.
- 511 (11) Fox, S. C.; Li, B.; Xu, D.; Edgar, K. J. Regioselective Esterification and Etherification of Cellulose: A Review. *Biomacromolecules*. June 13, 2011, pp 1956–1972. https://doi.org/10.1021/bm200260d.
- 514 (12) Sprung, M. M. *A SUMMARY OF THE REACTIONS OF ALDEHYDES WITH AMINES*. https://pubs.acs.org/sharingguidelines.
- 516 (13) Shen, Y.; Wang, Z.; Wang, Y.; Meng, Z.; Zhao, Z. A Self-Healing Carboxymethyl Chitosan/Oxidized Carboxymethyl Cellulose Hydrogel with Fluorescent Bioprobes for Glucose Detection. *Carbohydr Polym* **2021**, 274. https://doi.org/10.1016/j.carbpol.2021.118642.
- 520 (14) Strätz, J.; Liedmann, A.; Trutschel, M. L.; Mäder, K.; Groth, T.; Fischer, S. Development 521 of Hydrogels Based on Oxidized Cellulose Sulfates and Carboxymethyl Chitosan. *Cellulose* 522 **2019**, 26 (12), 7371–7382. https://doi.org/10.1007/s10570-019-02596-6.
- 523 George, D.; Maheswari, P. U.; Sheriffa Begum, K. M. M.; Arthanareeswaran, G. Biomass-524 Derived Dialdehyde Cellulose Cross-Linked Chitosan-Based Nanocomposite Hydrogel 525 with Phytosynthesized Zinc Oxide Nanoparticles for Enhanced Curcumin Delivery and 526 Bioactivity. JAgric Food Chem 2019, 67 (39),10880-10890. 527 https://doi.org/10.1021/acs.jafc.9b01933.
- 528 (16) Jeanes, A.; Wilham, C. A. Periodate Oxidation of Dextran. *J Am Chem Soc* **1950**, 72 (6), 2655–2657. https://doi.org/10.1021/ja01162a086.
- 530 (17) Xie, X.; Li, X.; Lei, J.; Zhao, X.; Lyu, Y.; Mu, C.; Li, D.; Ge, L.; Xu, Y. Oxidized Starch 531 Cross-Linked Porous Collagen-Based Hydrogel for Spontaneous Agglomeration Growth of 532 Adipose-Derived Stem Cells. *Materials Science and Engineering: C* 2020, 116, 111165. 533 https://doi.org/https://doi.org/10.1016/j.msec.2020.111165.
- 534 (18) Lyu, Y.; Yu, M.; Liu, Q.; Zhang, Q.; Liu, Z.; Tian, Y.; Li, D.; Changdao, M. Synthesis of 535 Silver Nanoparticles Using Oxidized Amylose and Combination with Curcumin for

- Enhanced Antibacterial Activity. *Carbohydr Polym* **2020**, 230. https://doi.org/10.1016/j.carbpol.2019.115573.
- 538 Sharma, P. K.; Taneja, S.; Singh, Y. Hydrazone-Linkage-Based Self-Healing and Injectable 539 Xanthan-Poly(Ethylene Glycol) Hydrogels for Controlled Drug Release and 3D Cell 540 Appl Mater Interfaces 2018. 10 (37),30936-30945. Culture. ACS 541 https://doi.org/10.1021/acsami.8b07310.
- Wang, S.; Oommen, O. P.; Yan, H.; Varghese, O. P. Mild and Efficient Strategy for Site-Selective Aldehyde Modification of Glycosaminoglycans: Tailoring Hydrogels with Tunable Release of Growth Factor. *Biomacromolecules* **2013**, *14* (7), 2427–2432. https://doi.org/10.1021/bm400612h.
- 546 (21) Wang, D.-A.; Varghese, S.; Sharma, B.; Strehin, I.; Fermanian, S.; Gorham, J.; Fairbrother, 547 D. H.; Cascio, B.; Elisseeff, J. H. Multifunctional Chondroitin Sulphate for Cartilage 548 Tissue–Biomaterial Integration. *Nat Mater* **2007**, *6* (5), 385–392. https://doi.org/10.1038/nmat1890.
- 550 (22) Jeon, O.; Alt, D. S.; Ahmed, S. M.; Alsberg, E. The Effect of Oxidation on the Degradation of Photocrosslinkable Alginate Hydrogels. *Biomaterials* **2012**, *33* (13), 3503–3514. https://doi.org/10.1016/j.biomaterials.2012.01.041.
- 553 (23) Balakrishnan, B.; Mohanty, M.; Umashankar, P. R.; Jayakrishnan, A. Evaluation of an in 554 Situ Forming Hydrogel Wound Dressing Based on Oxidized Alginate and Gelatin. 555 Biomaterials 2005, 26 (32), 6335–6342. 556 https://doi.org/10.1016/j.biomaterials.2005.04.012.
- 557 (24) Frasch, C. E. Preparation of Bacterial Polysaccharide–Protein Conjugates: Analytical and 558 Manufacturing Challenges. *Vaccine* **2009**, *27* (46), 6468–6470. https://doi.org/https://doi.org/10.1016/j.vaccine.2009.06.013.
- 560 (25) Chen, J.; Zhai, Z.; Edgar, K. J. Recent Advances in Polysaccharide-Based in Situ Forming 561 Hydrogels. *Curr Opin Chem Biol* **2022**, 70, 102200. 562 https://doi.org/https://doi.org/10.1016/j.cbpa.2022.102200.
- 563 (26) Kristiansen, K. A.; Potthast, A.; Christensen, B. E. Periodate Oxidation of Polysaccharides 564 for Modification of Chemical and Physical Properties. *Carbohydr Res* **2010**, *345* (10), 565 1264–1271. https://doi.org/https://doi.org/10.1016/j.carres.2010.02.011.
- Tao, H.; Lavoine, N.; Jiang, F.; Tang, J.; Lin, N. Reducing End Modification on Cellulose
 Nanocrystals: Strategy, Characterization, Applications and Challenges. *Nanoscale Horiz* 2020, 5 (4), 607–627. https://doi.org/10.1039/D0NH00016G.
- 569 (28) Heise, K.; Delepierre, G.; King, A. W. T.; Kostiainen, M. A.; Zoppe, J.; Weder, C.; Kontturi, E. Chemical Modification of Reducing End-Groups in Cellulose Nanocrystals. *Angewandte Chemie International Edition*. Wiley-VCH Verlag January 4, 2021, pp 66–87. https://doi.org/10.1002/anie.202002433.

- 573 (29) Hintze, V.; Schnabelrauch, M.; Rother, S. Chemical Modification of Hyaluronan and Their 574 Biomedical Applications. *Frontiers in Chemistry*. Frontiers Media S.A. February 11, 2022. 575 https://doi.org/10.3389/fchem.2022.830671.
- 576 (30) Bedini, E.; Laezza, A.; Iadonisi, A. Chemical Derivatization of Sulfated Glycosaminoglycans. *European Journal of Organic Chemistry*. Wiley-VCH Verlag June 1, 2016, pp 3018–3042. https://doi.org/10.1002/ejoc.201600108.
- 579 (31) Kim, D. H.; Kim, M.-D.; Choi, C.-W.; Chung, C.-W.; Ha, S. H.; Kim, C. H.; Shim, Y.-H.; 580 Jeong, Y.-I.; Kang, D. H. Antitumor Activity of Sorafenib-Incorporated Nanoparticles of Dextran/Poly(Dl-Lactide-Co-Glycolide) Block Copolymer. *Nanoscale Res Lett* **2012**, 7 (1), 91. https://doi.org/10.1186/1556-276X-7-91.
- Hashimoto, K.; Imanishi, S.-I.; Okada, M.; Sumitomo, H. Chemical Modification of the Reducing Chain End in Dextrans and Trimethylsilylation of Its Hydroxyl Groups; 1991.
- 585 (33) Solberg, A.; Mo, I. v.; Omtvedt, L. A.; Strand, B. L.; Aachmann, F. L.; Schatz, C.; Christensen, B. E. Click Chemistry for Block Polysaccharides with Dihydrazide and Dioxyamine Linkers A Review. *Carbohydr Polym* **2022**, *278*, 118840. https://doi.org/10.1016/J.CARBPOL.2021.118840.
- 589 (34) Guerry, A.; Cottaz, S.; Fleury, E.; Bernard, J.; Halila, S. Redox-Stimuli Responsive 590 Micelles from DOX-Encapsulating Polycaprolactone-g-Chitosan Oligosaccharide. 591 *Carbohydr Polym* **2014**, *112*, 746–752. 592 https://doi.org/https://doi.org/10.1016/j.carbpol.2014.06.052.
- 593 (35) Moussa, A.; Crépet, A.; Ladavière, C.; Trombotto, S. Reducing-End "Clickable" 594 Functionalizations of Chitosan Oligomers for the Synthesis of Chitosan-Based Diblock 595 Copolymers. *Carbohydr Polym* **2019**, 219, 387–394. 596 https://doi.org/https://doi.org/10.1016/j.carbpol.2019.04.078.
- (36) F-L Ho, F.; Klosiewicz, D. W. Proton Nuclear Magnetic Resonance Spectrometry for
 Determination of Substituents and Their Distribution in Carboxymethylcellulose; 1980;
 Vol. 52. https://pubs.acs.org/sharingguidelines.
- 600 (37) Stengel, D. B. Natural Products From Marine Algae Methods and Protocols Methods in Molecular Biology 1308. http://www.springer.com/series/7651.
- 602 (38) Perdih, P.; Čebašek, S.; Možir, A.; Žagar, E. Post-Polymerization Modification of Poly(L-603 Glutamic Acid) with D -(+)-Glucosamine. *Molecules* **2014**, *19* (12), 19751–19768. https://doi.org/10.3390/molecules191219751.
- Jones, A. X.; Cao, Y.; Tang, Y. L.; Wang, J. H.; Ding, Y. H.; Tan, H.; Chen, Z. L.; Fang, R. Q.; Yin, J.; Chen, R. C.; Zhu, X.; She, Y.; Huang, N.; Shao, F.; Ye, K.; Sun, R. X.; He, S. M.; Lei, X.; Dong, M. Q. Improving Mass Spectrometry Analysis of Protein Structures with Arginine-Selective Chemical Cross-Linkers. *Nat Commun* 2019, 10 (1). https://doi.org/10.1038/s41467-019-11917-z.

- 610 (40) Farkaš, P.; Bystrický, S. Efficient Activation of Carboxyl Polysaccharides for the 611 Preparation of Conjugates. *Carbohydr Polym* **2007**, *68* (1), 187–190. 612 https://doi.org/10.1016/j.carbpol.2006.07.013.
- (41) Zheng, X.; Gandour, R. D.; Edgar, K. J. Remarkably Regioselective Deacylation of
 Cellulose Esters Using Tetraalkylammonium Salts of the Strongly Basic Hydroxide Ion.
 Carbohydr Polym 2014, 111, 25–32.
 https://doi.org/https://doi.org/10.1016/j.carbpol.2014.04.014.
- 617 (42) Gao, C.; Liu, S.; Edgar, K. J. Regioselective Chlorination of Cellulose Esters by Methanesulfonyl Chloride. *Carbohydr Polym* **2018**, *193*, 108–118. https://doi.org/10.1016/j.carbpol.2018.03.093.
- 620 (43) Morris, K. F.; Johnson, C. S. Jr. Diffusion-Ordered Two-Dimensional Nuclear Magnetic 621 Resonance Spectroscopy. *J Am Chem Soc* **1992**, *114* (8), 3139–3141. 622 https://doi.org/10.1021/ja00034a071.
- (44) Zhong, Y.; Feng, Q.; Wang, X.; Yang, L.; Korovich, A. G.; Madsen, L. A.; Tong, R.
 Photocatalyst-Independent Photoredox Ring-Opening Polymerization OfO-Carboxyanhydrides: Stereocontrol and Mechanism. *Chem Sci* 2021, 12 (10), 3702–3712.
 https://doi.org/10.1039/d0sc05550f.
- 627 (45) Brus, J.; Urbanova, M.; Czernek, J.; Pavelkova, M.; Kubova, K.; Vyslouzil, J.; Abbrent, S.; Konefal, R.; Horský, J.; Vetchy, D.; Vysloužil, J.; Kulich, P. Structure and Dynamics of Alginate Gels Cross-Linked by Polyvalent Ions Probed via Solid State NMR Spectroscopy.

 630 Biomacromolecules 2017, 18 (8), 2478–2488. https://doi.org/10.1021/acs.biomac.7b00627.
- 631 (46) Manna, S. K.; Achar, T. K.; Mondal, S. Recent Advances in Selective Formaldehyde 632 Detection in Biological and Environmental Samples by Fluorometric and Colorimetric 633 Chemodosimeters. *Analytical Methods* **2021**, *13* (9), 1084–1105. 634 https://doi.org/10.1039/d0ay02252g.
- 635 (47) Fei Chen; Yafei Liu; Jianming Lu; Hwang, K. J.; Lee, V. H. L. A Sensitive Fluorometric 636 Assay for Reducing Sugars. *Life Sci* **1992**, *50* (9), 651–659. 637 https://doi.org/https://doi.org/10.1016/0024-3205(92)90252-K.
- You, S.; Kim, H.; Jung, H.; Kim, B.; Lee, E. J.; Kim, J. W.; Kim, Y. Tuning Surface Functionalities of Sub-10 Nm-Sized Nanocarriers to Target Outer Retina in Designing Drug Delivery Agents for Intravitreal Administration. *Biomaterials* 2020, 255, 120188. https://doi.org/https://doi.org/10.1016/j.biomaterials.2020.120188.
- 642 (49) Beecher, C. N.; Larive, C. K. 1H and 15N NMR Characterization of the Amine Groups of 643 Heparan Sulfate Related Glucosamine Monosaccharides in Aqueous Solution. *Anal Chem* 644 **2015**, 87 (13), 6842–6848. https://doi.org/10.1021/acs.analchem.5b01181.
- (50) Huang, K.-H.; Wei, Z.; Cooks, R. G. Accelerated Reactions of Amines with Carbon Dioxide
 Driven by Superacid at the Microdroplet Interface. *Chem Sci* 2021, *12* (6), 2242–2250.
 https://doi.org/10.1039/D0SC05625A.